THE JOURNAL OF PHYSICAL CHEMISTRY C
A JOURNAL OF THE AMERICAN CHEMICAL SOCIETY

pubs.acs.org/JPCC

Article

# Time-Resolved MIR Reflection–Absorption Spectroscopy of $N_2O$, CO, and $CH_4$ Adsorption on Graphene

Sefa Akça,* Laura v. Lüders, Georg S. Düsberg, Wolfgang Elsaesser, Norbert Nicoloso, and Ralf Riedel

Cite This: *J. Phys. Chem. C* 2023, 127, 4998–5003

Read Online

ACCESS | Metrics & More | Article Recommendations | Supporting Information

**ABSTRACT:** The time- and temperature-dependent adsorption of $N_2O$, CO, and $CH_4$ on CVD-grown graphene has been investigated by MIR reflection–absorption spectroscopy to gain information about the adsorption kinetics, notably the rate constants $k$ and activation energies $E_a$ of the adsorption step. The gas adsorption is followed by determining the change of the reflected beam intensity with time by taking difference spectra, i.e., subtracting the baseline signal (reflectivity of graphene at the respective gas excitation line) from the measurement with added gas. The experiments yield adsorption activation energies $E_a$ of $-19.6 \pm 1.1$ ($N_2O$), $-12.1 \pm 0.2$ (CO), and $-9.5 \pm 1.7$ kJ/mol ($CH_4$). The obtained $E_a$ values are in excellent agreement with the literature results from theory, thereby confirming these studies. The $E_a$ values indicate physisorption, i.e., no strong bonding of the gas molecules to graphene. The analyzed adsorption rate constants $k$ are reported for the first time and are on the order of $10^{11}$ to $10^{12}$ molecules·$s^{-1}$·$cm^{-2}$ with $N_2O$ showing the highest value and $CH_4$ the lowest value. The adsorption rate constants follow the series $N_2O$ > CO > $CH_4$, in line with the charge transfer abilities of the molecules. This work can be easily extended to kinetic studies of other gases hazardous to the environment and adsorption studies with other 2D materials using versatile MIR reflection–absorption spectroscopy.

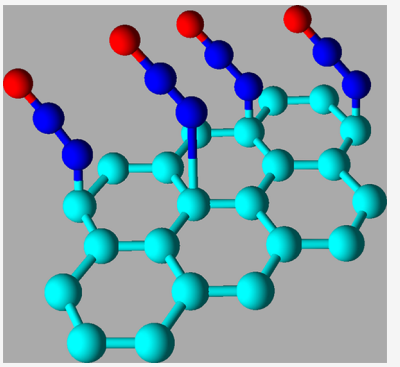



## INTRODUCTION

Fourier-transform IR spectroscopy is a fast and nondestructive measurement technique most commonly used as an analytical tool. The chemical bonds in a molecule exhibit vibrational modes whose energies reside in the infrared part of the spectrum. These modes are highly specific for a given molecule. Hence, determination of the transmitted or absorbed IR radiation provides the so-called fingerprint spectra of the material under investigation. Figure 1 shows the fingerprint lines of various gases in the midinfrared range (MIR). These fingerprint characteristics in the IR region of the spectrum are most commonly utilized as a qualitative analysis tool, though it is also possible to probe dynamic processes such as gas interactions on a surface, quantitative analysis of a chemical reaction, or the catalytic activity. However, due to the nature of the interferometer part in FTIR devices, there is always a trade-off between spectral and temporal resolution. Both of these parameters cannot be increased simultaneously, which is an important point of consideration when investigating dynamic processes. Therefore, it has to be decided in each analysis which resolution parameter is more crucial for the experiment.

This paper discusses the time-resolved MIR spectroscopy in a reflection–absorption configuration as a tool to probe the kinetics of the adsorption of the gas molecules $N_2O$, CO, and $CH_4$ on the surface of graphene as the temporal change of the surface concentration of gas molecules is inversely correlated with the intensity of the IR signal reflected from the gas–graphene interface (see, e.g., refs 2 and 3 for IR reflectivity/absorption data of graphene). The role of graphene in this time-resolved reflection–absorption measurement is 2-fold. (i) With its high specific surface area, it ensures a high concentration of adsorbed species. This high concentration of surface species allows measurement with low spectral resolution while still reaching excellent detection limits, allowing it to improve temporal resolution. (ii) Its very low IR absorption ensures that only information from the surface species is obtained.

A variety of surface-sensitive spectroscopic techniques may be used for gas kinetics studies besides FTIR. However, many of these methods require intricate experimental designs and/or conditions different from ambient atmosphere where most of the surface reactions happen. Time-resolved electronic detection may be suggested as an alternative to optical detection as the adsorption mechanisms tend to rely on charge transfer/doping processes of the monolayer material.[4] This effect has a large impact on the majority of 2D-based sensing applications and also has been used in gas sensors.[5] The latter lack the inherent selectivity necessary to follow the adsorption

**Received:** October 16, 2022
**Revised:** February 6, 2023
**Published:** March 2, 2023

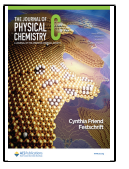




https://doi.org/10.1021/acs.jpcc.2c07277
*J. Phys. Chem. C* 2023, 127, 4998–5003

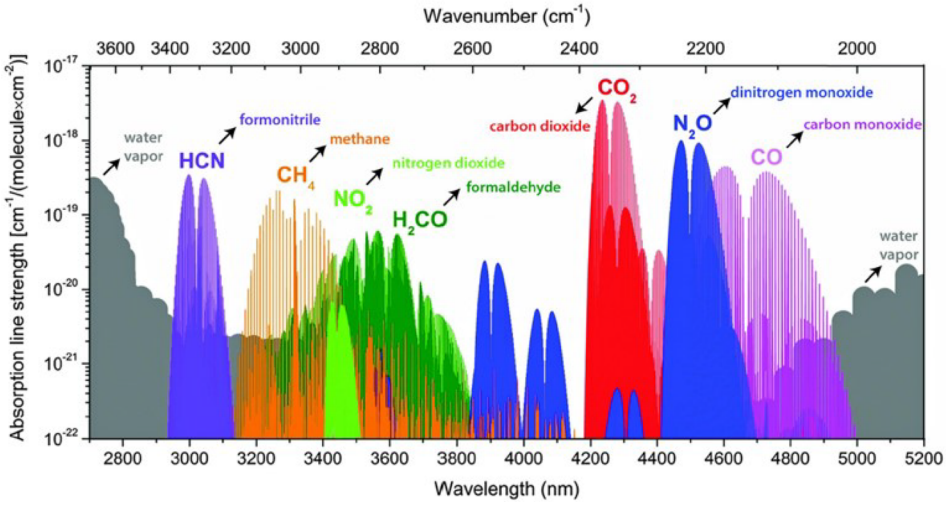


**Figure 1.** Overview of IR radiation absorption of typical gases in the MIR range. Reprinted with permission from ref 1. Copyright 2016 Royal Society of Chemistry.

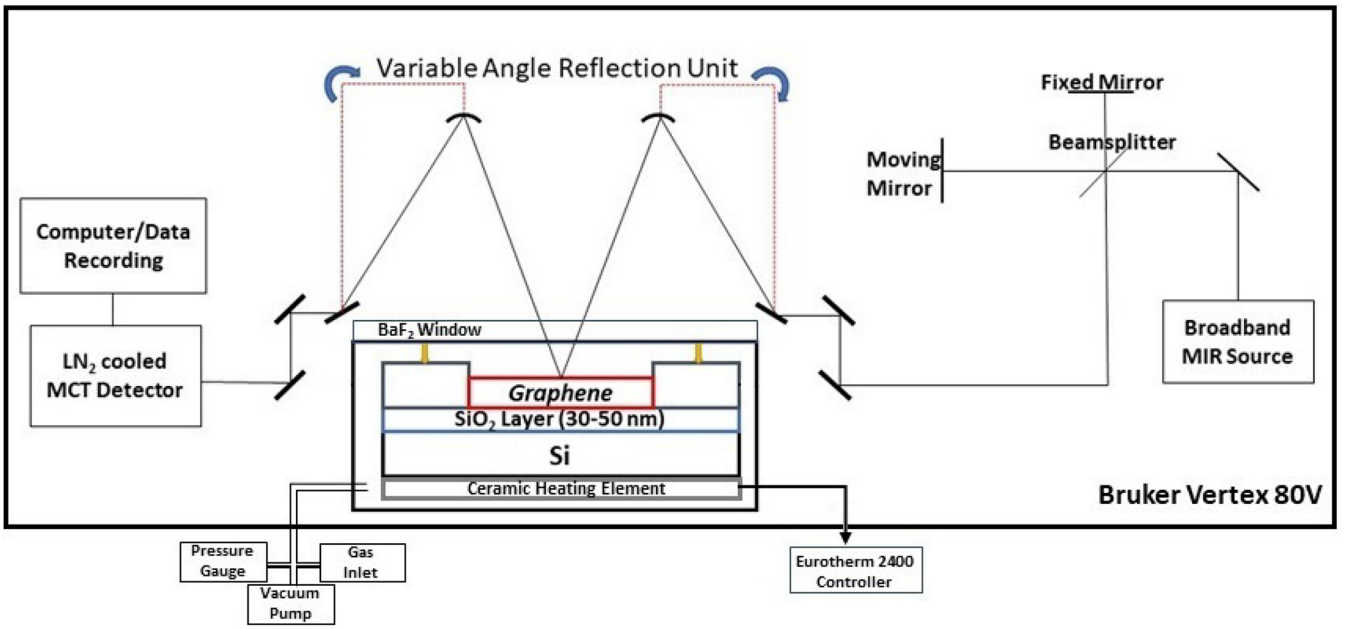


**Figure 2.** Schematic depiction of the homemade measurement setup depicting the FTIR beamline and IR reflection−absorption spectroscopy setup. Beamline of the Bruker Vertex 80V spectrometer is shown in a simplified manner.

of one and only one gas species. Notably, the impact of the ubiquitous presence of water molecules needs mentioning.[6] Gas detection with graphene as a sensor material is frequently used,[7−10] and typically, the gas adsorption step is fast in comparison to the desorption step. However, for sensoric purposes, mainly the correlation of the (steady state) sensor signal with the concentration of adsorbents matters, and therefore, analysis of the time-dependent sensor properties is usually out of the scope of such studies. Concerning gas sensing with optical techniques, it should be noted that real-time-resolved IR spectroscopy is not a novel approach. Yet, earlier work focused on desorption and necessitated complex experimental designs.[11,12] Recent advances employ modern IR laser sources (notably quantum cascade lasers) or hollow-waveguide cells.[13,14] They mainly try to improve on the detection limits under the application-specific conditions, whereas investigations of the gases desorbed from a concentrator preadsorption chamber attempt to circumvent challenges of the adsorption step. In contrast to experimental work, the theoretical research concentrates on gas−surface interfaces, providing structural features (bonding and charge transfer to/from a gas species) and calculation of adsorption/desorption activation energies ($E_a$). Concerning the wealth of gas species and substrate materials, reference to theoretical work is restricted here essentially to studies of graphene and $N_2O$, CO, and $CH_4$ as adsorbents.[15−18]

To conclude, MIR spectroscopy in a reflection−absorption configuration allows relatively easier experimental design and possesses inherent selectivity toward the target gases, and the high spectral resolution combined with the high specific surface area of graphene as the adsorbing medium enables excellent sensitivity toward surface-adsorbed species. Additionally, real-time temporal resolution instead of stepwise measurements provides kinetic studies with unprecedented precision.



https://doi.org/10.1021/acs.jpcc.2c07277
J. Phys. Chem. C 2023, 127, 4998−5003

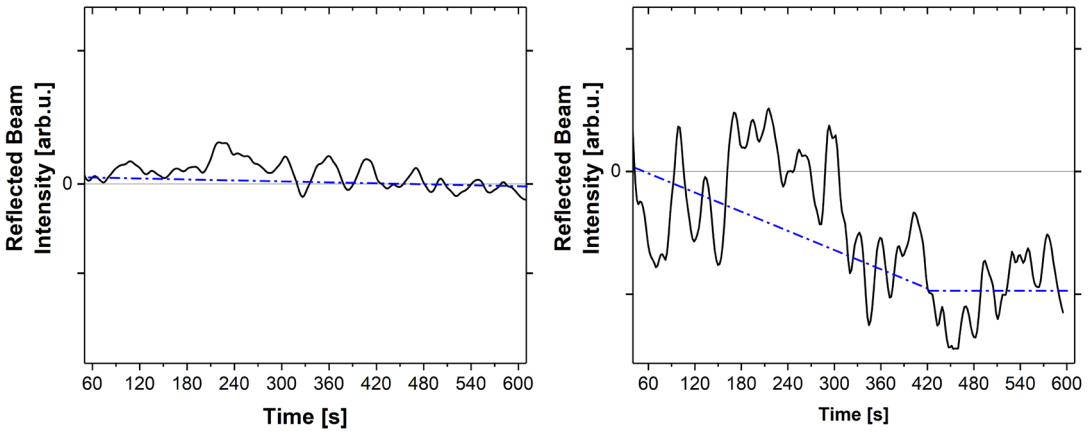


**Figure 3.** Reflected beam intensity (difference spectrum) at 2195−2205 $cm^{-1}$ for the adsorption of $N_2O$ on graphene at constant temperature: $T$ = 300 (left) and 135 °C (right). Total measurement time of 600 s with gas dose introduced at 30 s. Scale of axes on both plots are identical, and zero point in the $y$ axes of difference spectra corresponds to the point where the actual measurement and the baseline signals are equal. Negative trends in the plot on the right indicate a decrease on reflected beam intensity/increase in the IR absorption and hence increase in the $N_2O$ concentration on the surface.

Apart from providing the adsorption rate constants of $N_2O$, CO, and $CH_4$ on graphene, the main aim of the study is to corroborate/disapprove the theoretical studies given in the literature of said gases interacting with graphene.

## EXPERIMENTAL SECTION

The experimental part is comprised of a description of the materials, the measurement setup, the pretreatment and background correction steps of a MIR measurement, as well as a brief depiction of the adsorption experiment at constant/variable temperature using difference spectra. Details about the pretreatment and the background correction of the MIR experiment are given in Supporting Information S1 and S2.

**Materials and Measurement Setup.** Nitrous oxide and methane were acquired from Messer Industriegase GmbH (Bad Soden, Germany). Carbon monoxide and nitrogen (used for flushing the chamber) were acquired from Air Liquide GmbH (Düsseldorf, Germany). Gas flow control was ensured through a MKS 119C flow rate controller with a MKS 647C power supply (Munich, Germany). The graphene was grown on 25 $\mu$m thick Cu foils (Alfa Aesar, 99.8%) via chemical vapor deposition (CVD) using a 2:1 ratio mixture of $H_2$ and $CH_4$.[19] The quality of the graphene sample was determined by Raman spectroscopy, atomic force microscopy (AFM), and scanning electron microscopy (SEM). A Raman 2D/G intensity ratio of ∼2 as well as low fwhm values of the G and 2D peaks (<15 and 30 $cm^{-1}$) indicate high-quality few-layer graphene with ∼1.5 × $10^{13}$ $cm^{-2}$ Raman-active defects (see also ref 20). A typical Raman spectrum and mapping is given in Supporting Information S3, together with further information about the graphene sample preparation and the characterization by AFM and SEM.

Figure 2 provides a schematic depiction of the measurement setup. The measurement chamber ($V \approx 65$ $cm^3$) housing the graphene sample was designed and manufactured in house. A $BaF_2$ single crystal (85 × 35 × 6 $mm^3$), sealed by an O ring to the chamber, was used as IR-transparent window (∼90% transmission in the IR range given in this work). It was provided by Hellma Optic GmbH (Jena, Germany). The ceramic heating element inside the chamber ($T_{max}$ = 500 °C) was acquired from Bach RC (Seefeld, Germany). Two thermocouples and a Eurotherm 2400 controller (Limburg an der Lahn, Germany) were used to measure/control the temperature of the heating element and the thereon mounted graphene sample.

FTIR measurements in reflection−absorption mode were performed with a Bruker Vertex 80V FTIR spectrometer (Bruker Optics, Ettlingen). Spectra were recorded in the spectral range of 4000−500 $cm^{-1}$ with a spectral resolution of 0.25 $cm^{-1}$. The temporal resolution of the time-resolved IR spectra was 1 ± 0.1 $s^{-1}$.

**Adsorption Experiment at Constant/Variable Temperature.** The time-resolved adsorption experiments were done in two steps. Both steps are identical with the exception of step 1 which was carried out at the same experimental conditions as step 2 but without any target gas in the chamber. Step 1 provides the baseline in the evaluation of the adsorption data, allowing one to eliminate, e.g., temperature-dependent changes of the reflectivity of graphene. In the second step, the graphene sample is first heated to the respective starting temperature (typically 300 °C) under vacuum ($p \approx 10^{-5}$ mbar). Valves on the vacuum line are closed to seal off the chamber followed by the simultaneous start of the beamline and data acquisition. Thirty seconds later the desired gas is introduced into the chamber with a flow rate of 50 sccm for a total duration of 10 s. Waiting for about 10 min ensures that the gas is well distributed inside the chamber. This experimental procedure is followed in the adsorption measurements at constant and variable temperature. In the latter case, the temperature is steadily reduced by typically 0.35 $K \cdot s^{-1}$, causing a continuous increase of adsorbed gas molecules on the graphene surface, directly correlated with the decrease of the reflected beam intensity (of the respective gas line) at the graphene interface.

## RESULTS AND DISCUSSION

The results will be discussed in two parts. First, experiments at constant temperature will be shown for $T$ = 300 and 135 °C, i.e., the highest and lowest target temperature of an experiment. The upper limit has been chosen to avoid degradation of the graphene surface by traces of oxygen/water in the target gas. The lower value is set to temperature > 100 °C to avoid the formation of a water layer/water spots on graphene during cooling of the sample. In the second part,


https://doi.org/10.1021/acs.jpcc.2c07277
J. Phys. Chem. C 2023, 127, 4998−5003

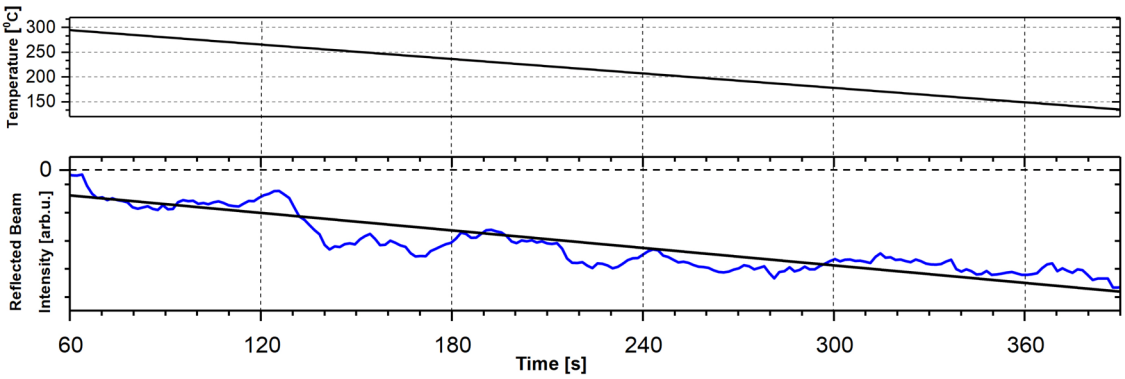


**Figure 4.** Temperature-induced adsorption of $N_2O$ on graphene. Applied temperature profile (top) and reflected beam intensity (difference spectrum) at 2195−2205 $cm^{-1}$ (bottom). Clear negative trend in the reflected beam intensity indicates increasing IR absorption by $N_2O$/an increase in its concentration on the graphene surface.

time-resolved reflection−absorption data obtained on cooling from $T_{target}$ to $T$ = 135 °C are presented.

**Adsorption at Constant Temperature.** Gas adsorption at constant temperature has been investigated to check whether the thermodynamic equilibrium between molecules in the gas phase and adsorbed molecules is reached within the applied measuring time, typically about 10 min. Figure 3 shows the adsorption of $N_2O$ at $T$ = 300 and 135 °C as a function of time. These data are obtained via the two-step process explained in the Experimental Section and are presented as difference spectra, i.e., by subtraction of the graphene reflectivity without added gases at exactly the same conditions as the measurement with added gas. The figure on the left (300 °C) shows a time-independent progression, indicating that the steady state has already been reached at the beginning of the experiment. The fact that the difference signal is quite small further suggests that very few, if any, $N_2O$ molecules are adsorbed on graphene at $T$ = 300 °C. $H_2O$ is also not adsorbed at this temperature.[6] Accordingly, the concentration of adsorbed $N_2O$ at $T$= 300 °C can be set to zero at these conditions.

The right side of Figure 3 presents the difference spectrum of $N_2O$ at $T$ = 135 °C. A clear decrease of the reflected beam intensity is observed at the beginning of the experiment which tends to flatten out, suggesting that the $N_2O$ concentration on graphene increases with time, approaching a steady state after about 400−600 s.

**Temperature-Induced Adsorption.** A typical temperature-induced adsorption experiment with $N_2O$ is presented in Figure 4. A continuous decrease in the measured reflected beam intensity is seen, tantamount to an increase of gas adsorption on graphene with time. A similar behavior is observed for the other two investigated gases with $CH_4$ showing the least change (see Supporting Information S4). Two important kinetic parameters of the adsorption process can be derived from this data: rate constants $k$ and adsorption activation energies $E_a$. As mentioned above, the concentration of adsorbed species is approximately zero at the start of the experiment at $T$ = 300 °C. The concentration at the end of the experiment (at $T$ = 135 °C) corresponds to $[c]_{end}$. The intensity change of the reflected beam with time—equivalent to the concentration change $([c]_x - [c]_0)/([c]_0 - [c]_{end})$ over time—delivers the rate constants $k$. The concentration at the end of the experiment can be also expressed as a quantitative number by the following estimate. With the atomic density of 3.82 × $10^{15}$ $cm^{-2}$ of graphene and every third carbon atom considered as an adsorption site, the number of adsorbed molecules under the beam spot (diameter of 0.05 cm) is calculated as 7.85 × $10^{13}$ $cm^{-2}$. The calculated number of adsorbed molecules on the graphene surface is, of course, a rough estimate neglecting, e.g., multilayer formation on the graphene surface and multiple reflections of the beam at the graphene/$SiO_2$ interface. It provides, however, the first information about the sensitivity of the experiment (~$10^{14}$ molecules/$cm^2$ and even lower surface concentrations).

The adsorption rate depends on temperature and the $k$ values, taken from Figure 4 at a respective temperature $T$, and can be used to determine the activation energy $E_a$ of the adsorption step. Figure 5 provides the activation energy of the

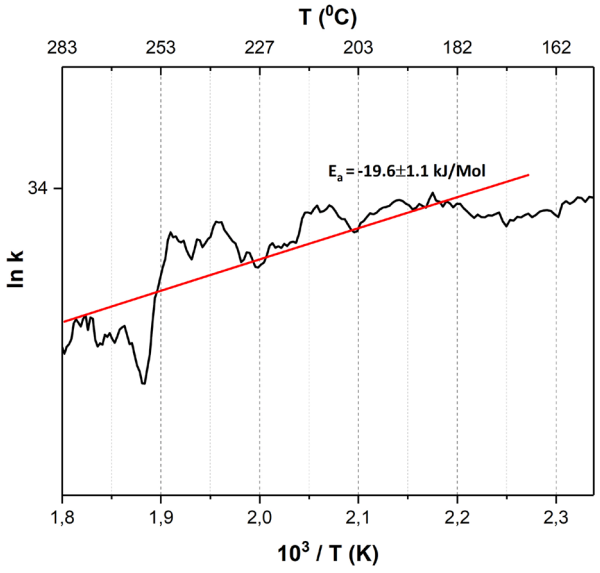


**Figure 5.** Arrhenius plot for the adsorption of $N_2O$ on graphene.

adsorption of $N_2O$ by plotting ln $k$ vs $1/T$ (Arrhenius plot). Arrhenius plots of the other two gases are presented on the Supporting Information. Table 1 lists the obtained $k$ and $E_a$ values of $N_2O$, CO, and $CH_4$ together with literature data. All $E_a$ values of this work agree with the literature within a margin of <15%, with $N_2O$ showing the highest adsorption energy and $CH_4$ exhibiting the lowest. The experimental data corroborate the literature DFT simulations of the gas−graphene interface. According to the literature, CO bonding relies heavily on the doping state of graphene.[17] For nondoped graphene, theory



https://doi.org/10.1021/acs.jpcc.2c07277
J. Phys. Chem. C 2023, 127, 4998−5003

Table 1. Adsorption Rate Constants, $k$, and Adsorption Activation Energies, $E_a$, Derived from FTIR Difference Spectra

| gas | rate constant, $k$ (molecules·s$^{-1}$·cm$^{-2}$) | adsorption $E_a$ (kJ/mol) | literature values $E_a$ (kJ/mol) |
|---|---|---|---|
| $N_2O$ | $10.8 \pm 0.3 \times 10^{11}$ | $-19.6 \pm 1.1$ | $-19.29$, $-17.36$[16] |
| CO | $4.5 \pm 0.3 \times 10^{11}$ | $-12.1 \pm 0.2$ | $-0.96$, $-6.75$, $-12.53$[17,18] |
| $CH_4$ | $3.0 \pm 0.5 \times 10^{11}$ | $-9.5 \pm 1.7$ | $-12.09$[15] |

suggests an extremely weak interaction ($E_a$ = −0.96 kJ/mol). Virtually defect-free graphene is, however, an ideal material, and the cited value for p-doped graphene ($E_a$ = −12.5 kJ/mol) closely agrees with our experimental value of 12.1 ± 0.2 kJ/mol. Lastly, it should be noted that $CH_4$ shows a lower $E_a$ value, while $N_2O$ and CO exhibit higher adsorption activation energies than the cited theoretical values. This behavior probably originates from the different charge transfer abilities of the investigated molecules. As $CH_4$ is a nonpolar molecule, it should not induce any significant charge transfer, whereas adsorption of $N_2O$ and CO causes, respectively, p and n doping of graphene. In-situ optical and electrical measurements can shine more light on this difference and are in progress.

## SUMMARY

Time-resolved MIR reflection−absorption spectroscopy on a graphene surface has been used to probe the adsorption kinetics of $N_2O$, CO, and $CH_4$. To this end, a purpose-built chamber with a $BaF_2$ single-crystal window has been mounted to a Bruker Vertex 80V Spectrometer. Using CVD-grown graphene (on Si) as the reflecting part, we could determine the adsorption of gases with a detection limit of $\leq 10^{14}$ molecules·cm$^{-2}$. The adsorption activation energies, $E_a$, for said gases are found to be within close agreement with the theoretical values. The $E_a$ values indicate weak chemical bonding to graphene. The adsorption strength follows the series $N_2O$ > CO > $CH_4$ and mirrors the charge transfer abilities of the molecules. The rate constants, $k$, are on the order of $10^{11}$−$10^{12}$ molecules·cm$^{-2}$·s$^{-1}$, exhibiting the highest uncertainty in the case of $CH_4$ due to the comparatively low intensity of the reflected beam in the adsorption experiment. MIR reflection−absorption spectroscopy might be extended to other environmentally hazardous or commercially relevant gases as well as other 2D materials to get a more comprehensive view on the kinetic properties of 2D material/gas interfaces.

## ASSOCIATED CONTENT

### Supporting Information

The Supporting Information is available free of charge at https://pubs.acs.org/doi/10.1021/acs.jpcc.2c07277.

FTIR spectroscopy spectra of CO on 1−3 layer graphene, Raman spectroscopy of 1−3 layer graphene, Raman 2D/G intensity ratio map, AFM surface mapping and step height measurement of the graphene sample, SEM image of the graphene sample, MIR reflection−absorption difference spectra of CO and $CH_4$ adsorption on graphene and resulting Arrhenius plots (PDF)

## AUTHOR INFORMATION


### Corresponding Author

**Sefa Akça** − *Institute of Material and Geosciences, Technical University of Darmstadt, 64287 Darmstadt, Germany;* orcid.org/0000-0003-2930-5177; Email: sefa.akca@stud.tu-darmstadt.de

### Authors

**Laura v. Lüders** − *Institute of Physics, University of the Bundeswehr Munich, 85577 Neubiberg, Germany*

**Georg S. Düsberg** − *Institute of Physics, University of the Bundeswehr Munich, 85577 Neubiberg, Germany;* orcid.org/0000-0002-7412-700X

**Wolfgang Elsaesser** − *Institute of Applied Physics, Technical University of Darmstadt, 64289 Darmstadt, Germany*

**Norbert Nicoloso** − *Institute of Material and Geosciences, Technical University of Darmstadt, 64287 Darmstadt, Germany*

**Ralf Riedel** − *Institute of Material and Geosciences, Technical University of Darmstadt, 64287 Darmstadt, Germany*

Complete contact information is available at: https://pubs.acs.org/10.1021/acs.jpcc.2c07277


### Notes

The authors declare no competing financial interest.

## ACKNOWLEDGMENTS

The authors thank Dr. Andreas Herdt for his suggestions regarding the optical setup as well as his help with Matlab and Michael Weber for his assistance during design and construction of the setup. L.v.L and G.S.D. thank the European Union's Horizon 2020 Research and Innovation Programme under grant agreement no. 881603 (Graphene Flagship) for financial support. Further we thank the dtec.bw - Digitalization and Technology Research Center of the Bundeswehr. dtec.bw is funded by the European Union- NextGenerationEU. Funding by the Deutsche Forschungsgemeinschaft (DFG) is gratefully acknowledged (Grant No. RI 510/68-1)

## REFERENCES


(1) Vainio, M.; Halonen, L. Mid-infrared optical parametric oscillators and frequency combs for molecular spectroscopy. *Phys. Chem. Chem. Phys.* **2016**, *18*, 4266−4294.

(2) Santos, C. N.; Joucken, F.; De Sousa Meneses, D.; Echegut, P.; Campos-Delgado, J.; Louette, P.; Raskin, J. P.; Hackens, B. Terahertz and mid-infrared reflectance of epitaxial graphene. *Sci. Rep.* **2016**, *6*, 24301.

(3) Yan, H.; Xia, F.; Zhu, W.; Freitag, M.; Dimitrakopoulos, C.; Bol, A. A.; Tulevski, G.; Avouris, P. Infrared spectroscopy of wafer-scale graphene. *ACS Nano* **2011**, *5*, 9854−9860.

(4) Lee, K.; Gatensby, R.; McEvoy, N.; Hallam, T.; Duesberg, G. S. High-performance sensors based on molybdenum disulfide thin films. *Adv. Mater.* **2013**, *25*, 6699−6702.

(5) Kim, H. Y.; Lee, K.; McEvoy, N.; Yim, C.; Duesberg, G. S. Chemically modulated graphene diodes. *Nano Lett.* **2013**, *13*, 2182−2188.

(6) Minami, T.; Ochi, S.; Nakai, H.; Kinoshita, T.; Ohno, Y.; Nagase, M. Thermal desorption of structured water layer on epitaxial graphene. *AIP Adv.* **2021**, *11*, 125012.

(7) Chen, Z.; Wang, J.; Wang, Y. Strategies for the performance enhancement of graphene-based gas sensors: A review. *Talanta* **2021**, *235*, 122745.

(8) Wang, C.; Wang, Y.; Yang, Z.; Hu, N. Review of recent progress on graphene-based composite gas sensors. *Ceram. Int.* **2021**, *47*, 16367−16384.

(9) Basu, S.; Bhattacharyya, P. Recent developments on graphene and graphene oxide based solid state gas sensors. *Sensors and Actuators, B: Chemical* **2012**, *173*, 1−21.
(10) Yuan, W.; Shi, G. Graphene-based gas sensors. *Journal of Materials Chemistry A* **2013**, *1*, 10078−10091.
(11) Borguet, E.; Dai, H. L. Time-resolved surface kinetics by IR diode laser reflection-absorption spectroscopy. *J. Electron Spectrosc. Relat. Phenom.* **1990**, *54*−*55*, 573−580.
(12) Fonseca, A. A.; Gardner, P.; Torbati, R.; Sakakini, B. H.; Waugh, K. C. The determination of desorption rate constants by monitoring of the time dependence of the decay of infrared bands - Dynamic infrared spectroscopy. *J. Catal.* **2004**, *221*, 313−318.
(13) Da Silveira Petruci, J. F.; Wilk, A.; Cardoso, A. A.; Mizaikoff, B. A Hyphenated Preconcentrator-Infrared-Hollow-Waveguide Sensor System for N2O Sensing. *Sci. Rep.* **2018**, *8*, 5909.
(14) Kasyutich, V. L.; Holdsworth, R. J.; Martin, P. A. Mid-infrared laser absorption spectrometers based upon all-diode laser difference frequency generation and a room temperature quantum cascade laser for the detection of CO, N2O and NO. *Applied Physics B: Lasers and Optics* **2008**, *92*, 271−279.
(15) Vekeman, J.; G. Cuesta, I.; Faginas-Lago, N.; Wilson, J.; Sanchez-Marin, J.; Sanchez de Meras, A. Potential models for the simulation of methane adsorption on graphene: Development and CCSD(T) benchmarks. *Phys. Chem. Chem. Phys.* **2018**, *20*, 25518−25530.
(16) Vakili, M.; Gholizadeh, R.; Ghadi, A.; Salmasi, E.; Sinnokrot, M. Computational investigation of N2O adsorption and dissociation on the silicon-embedded graphene catalyst: A density functional theory perspective. *Journal of Molecular Graphics and Modelling* **2020**, *101*, 107752.
(17) Wang, W.; Zhang, Y.; Shen, C.; Chai, Y. Adsorption of CO molecules on doped graphene: A first-principles study. *AIP Adv.* **2016**, *6*, 025317.
(18) Yang, S.; Lei, G.; Xu, H.; Xu, B.; Li, H.; Lan, Z.; Wang, Z.; Gu, H. A DFT study of CO adsorption on the pristine, defective, In-doped and Sb-doped graphene and the effect of applied electric field. *Appl. Surf. Sci.* **2019**, *480*, 205−211.
(19) McManus, J. B.; Hennessy, A.; Cullen, C. P.; Hallam, T.; McEvoy, N.; Duesberg, G. S. Controlling Defect and Dopant Concentrations in Graphene by Remote Plasma Treatments. *Phys. Status Solidi B* **2017**, *254*, 1700214.
(20) Shlimak, I.; Kaveh, M. Raman Spectra in Irradiated Graphene: Line Broadening, Effects of Aging and Annealing. *Graphene* **2020**, *09*, 13−28.





https://doi.org/10.1021/acs.jpcc.2c07277
*J. Phys. Chem. C* 2023, 127, 4998−5003